# Characteristics and mixing state of amine-containing particles at a rural site in the Pearl River Delta, China.

Chunlei Cheng[1,2], Zuzhao Huang[3], Chak K. Chan[4], Yangxi Chu[4], Mei Li[1,2]*, Tao Zhang[5], Yubo Ou[5], Duohong Chen[5], Peng Cheng[1,2], Lei Li[1,2], Wei Gao[1,2], Zhengxu Huang[1,2], Bo Huang[1,2,6], Zhong Fu[6], Zhen Zhou[1,2]*

[1]Institute of Mass Spectrometer and Atmospheric Environment, Jinan University, Guangzhou 510632, China

[2]Guangdong Provincial Engineering Research Center for on-line source apportionment system of air po llution, Guangzhou 510632, China

[3]Guangzhou Environmental Technology Assessment Center, Guangzhou 510045, China

[4]School of Energy and Environment, City University of Hong Kong, Hong Kong, China

[5]State Environmental Protection Key Laboratory of Regional Air Quality Monitoring, Guangdong Environmental Monitoring Center, Guangzhou 510308, China

[6]Guangzhou Hexin Analytical Instrument Limited Company, Guangzhou 510530, China

*Correspondence to*: Mei Li (limei2007@163.com) and Zhen Zhou (zhouzhen@gig.ac.cn)

Tel: 86-20-85225991, Fax: 86-20-85225991

**Abstract.** Particulate amines play an important role for the particle acidity and hygroscopicity and also contribute to secondary organic aerosol mass. We investigated the sources and mixing states of particulate amines using a single-particle aerosol mass spectrometer (SPAMS) during summer and winter 2014 at a rural site in the Pearl River Delta, China. Amine-containing particles accounted for 11.1 % and 9.4 % of the total detected individual particles in summer and winter, respectively. Although the increase of amine-containing particle count mostly occurred at night, no obvious correlations between amine-containing particles and ambient relative humidity (RH) were found during the sampling period. Among the three markers we considered, the most abundant amine marker was $^{74}(C_2H_5)_2NH_2^+$, which was detected in 90% and 86% of amine-containing particles in summer and winter, followed by amine marker ions of $^{59}(CH_3)_3N^+$, and $^{86}(C_2H_5)_2NCH_2^+$ which were detected in less than 10% of amine-containing particles during sampling period. The amine-containing particles were characterized by high fractions of carbonaceous marker ions, carbon-nitrogen fragments, sulfate and nitrate in both summer and winter. More than 90% of amine-containing particles were found to be internally mixed with sulfate throughout the sampling period, while the percentage of amine particles containing nitrate increased from 43% in summer to 69% in winter. Robust correlations between the peak intensities of amines and the sum of nitrate and sulfate were observed, suggesting the possible formation of aminium sulfate and nitrate salts. Interestingly, only 8% of amine particles contained ammonium in summer, while the percentage increased dramatically to 54 % in winter, indicating a relatively ammonium-poor state in summer and an ammonium-rich state in winter. The total ammonium-containing particles were investigated and showed a much lower abundance in ambient particles in summer (3.6%) than that in winter (32.6%), which suggests the ammonium-poor state of amine-containing particles in summer may be related to the lower abundance of ammonia/ammonium in gas and particle phase. In addition, higher abundance of amines in ammonium-containing particles than that of ammonium in amine-containing particles suggests a possible contribution of ammonium–amine exchange reactions to the low abundance of ammonium in amine-containing particles

at high ambient RH (72 ± 13 %) in summer. The particle acidity of amine-containing particles is estimated via the relative acidity ratio ($R_a$), which is defined as the ratio of the sum of the sulfate and nitrate peak areas divided by the ammonium peak area. The $R_a$ was 326 ± 326 in summer and 31 ± 13 in winter, indicating that the amine-containing particles were more acidic in summer than in winter. However, after including amines along with the ammonium in the acidity calculation, the new $R_a$' values showed no seasonal change in summer (11 ± 4) and winter (10 ± 2), which suggests that amines could be a buffer for the particle acidity of ammonium-poor particles.

**Keywords**: Amine; Single particles; Mixing state; Aminium salts; Particle acidity; SPAMS.

## 1 Introduction

Amines, a group of nitrogen-containing organic compounds, are ubiquitous in the atmospheric gas and particle phases (Ge et al., 2011b). A variety of low molecular weight (LMW) aliphatic amines have been detected in emissions from anthropogenic and natural sources, including animal husbandry, biomass burning, industrial emissions, vehicle exhaust, and marine sources (Rogge et al., 1994;Rappert and Muller, 2005;Calderon et al., 2007;Ngwabie et al., 2007;Ge et al., 2011b). LMW aliphatic amines have gas-phase concentrations two orders of magnitude lower than that of ammonia ($NH_3$) (Sorooshian et al., 2008), but are more alkaline than $NH_3$ (Ge et al., 2011a). Due to their strong basicity and water solubility, LMW amines can undergo acid-base reactions with sulfuric and nitric acid to form aminium salts (Angelino et al., 2001;Sorooshian et al., 2007;Pratt et al., 2009), which has been found to enhance new particle formation beyond the amounts produced from reactions between acids and $NH_3$ alone (Kurten et al., 2008;Berndt et al., 2010;Place et al., 2010;Wang et al., 2010). In addition, once partitioned into the particle phase, these LMW aliphatic amines can enhance aerosol particle hygroscopicity (Chu et al., 2015;Sauerwein et al., 2015). Furthermore, amines can be oxidized by OH radicals, $NO_3$ radicals, and $O_3$ in the atmosphere to form semi-volatile and non-volatile

compounds, some of which are highly toxic (Lee and Wexler, 2013), and which contribute to secondary organic aerosol (SOA) mass (Murphy et al., 2007;Malloy et al., 2009).

The mass concentration and temporal distribution of LMW aliphatic amines in aerosols have been studied extensively in a variety of environments, and LMW aliphatic amines account for 2–12 % of organic mass (Day et al., 2009;Gilardoni et al., 2009;Liu et al., 2009;Russell et al., 2009;Williams et al., 2010). In recent years, real-time single particle mass spectrometry has been used to measure the size and chemical composition of individual amine-containing particles with high time resolution. The mixing state and single-particle characteristics of amines have been investigated in laboratory and field environments (Angelino et al., 2001;Moffet et al., 2008;Silva et al., 2008;Pratt et al., 2009;Huang et al., 2012;Zhang et al., 2012). Pratt et al. (2009) studied seasonal differences in aminium and ammonium salts on a single-particle basis using an aerosol time-of-flight mass spectrometer (ATOFMS) coupled with a thermodenuder and reported that the gas-to-particle partitioning of amines is dependent on particle acidity. Healy et al. (2015) investigated the temporal distributions of alkylamines at five European sites, and found that alkylamines were internally mixed with both sulfate and nitrate, which suggests that the formation of aminium salts was important at all sites. Zauscher et al. (2013) detected strong signals of amine marker ($^{86}(C_2H_5)_2NCH_2^+$) in biomass burning aerosols associated with the increase of ambient relative humidity, indicating the direct emission of amines from biomass burning and the important influence of high RH (>90%) on the partitioning process of amines. Huang et al. (2012) determined the mixing state of amine-containing particles in Shanghai and found higher number concentrations of amine-containing particles in winter than in summer, which they attributed to effective acid-base reactions between sulfuric acid and amines under low-temperature, high-RH conditions. Zhang et al. (2012) measured trimethylamine-containing particles in Guangzhou and found preferential trimethylamine gas-to-particle partitioning during fog events. These field observations emphasize the important role of acid-base reactions in the partitioning of amines from the gas phase to the particle

phase. Recent laboratory studies have revealed that the exchange between amine gases and particulate $NH_3$ and/or ammonium also contributes substantially to amine content and results in a depletion of $NH_3$ and/or ammonium in the particle phase (Lloyd et al., 2009;Bzdek et al., 2010;Qiu et al., 2011;Liu et al., 2012;Chan and Chan, 2013;Chu and Chan, 2016, 2017;Sauerwein and Chan, 2017); however, the significance of such exchange reactions in the ambient environment has not been fully explored. Therefore, the influence of ammonia and particle acidity on the distribution of amines in the particle phase should be studied comprehensively through field measurements.

The aim of this study was to investigate the mixing state of a series of LMW aliphatic amines with sulfate, nitrate, and ammonium in individual particles using a single-particle aerosol mass spectrometer (SPAMS) at a rural site in the Pearl River Delta, China. In order to explore amine origins and gas-to-particle partitioning processes, amine-containing particles from both summer and winter were classified into three types based on mass spectral patterns. The aminium sulfate and nitrate salt formation processes and internal mixing state with ammonium were used to deduce the relationship between amines and ammonium in the particle phase and the influence of amines on particle acidity.

# 2 Methods

## 2.1 Aerosol sampling

Ambient single particles were collected and analyzed using a SPAMS at the Guangdong Atmospheric Supersite (22.73° N, 112.93° E), a rural site in Heshan City in the Pearl River Delta (PRD), China (Figure S1). The sampling site is surrounded by villages and experiences little influence from local industrial emissions (Cheng et al., 2017). The SPAMS was installed at the top of the main building, and aerosols were introduced to the SPAMS through a 2.5 m copper tube. SPAMS sampling was conducted continuously from 18 July to 1 August 2014 and from 27 January to 8 February 2015; several hours of data are missing due to technical maintenance. During the sampling period, hourly $O_3$ concentrations were measured using an $O_3$

analyzer (model 49i, Thermo Scientific). Meteorological data, including temperature, relative humidity, wind speed, and wind direction, were also measured during SPAMS sampling.

### 2.2 SPAMS

SPAMS was designed by the Guangzhou Hexin Analytical Company based on preexisting ATOFMS principles (Prather et al., 1994;Noble and Prather, 1996). The setup and design of the SPAMS has been detailed previously (Li et al., 2011). Briefly, single particles are sampled through an 80 μm critical orifice into the aerodynamic lens at a flow rate of 75 ml $min^{-1}$. Then, the particles pass consecutively through two laser beams (diode Nd:YAG, 532 nm) spaced 6 cm apart, and the aerodynamic diameter of the single particle is calculated using the particle flight time and velocity between the two laser beams. The single particle velocity is also used to calculate the precise time at which to fire the desorption and ionization laser (Nd:YAG laser, 266nm), which is positioned 12 cm downstream from the second laser beam. After ionization, the positive and negative ions are detected by a Z-shaped bipolar time-of-flight mass spectrometer. In this work, the ionization laser pulse energy was 0.6 mJ and the power density was $1.06 \times 10^8$ W $cm^{-2}$ throughout the campaign. The size range of single particles detected by SPAMS ranged from 0.2 to 2 μm, calibrated with standard polystyrene latex spheres (Nanosphere size standards, Duke Scientific Corp., Palo Alto) of 0.22–2.0 μm diameter before and after the campaign (Cheng et al., 2017).

### 2.3 Data analysis

Particle size and chemical composition were obtained via SPAMS mass spectral analysis using the Computational Continuation Core (COCO; version 3.0) toolkit in Matlab. According to the field studies of ATOFMS and SPAMS, it is difficult to accurately determine the number concentration of ambient particles using SPAMS alone due to the size-dependent transmission efficiencies of particles through aerodynamic lens and composition dependent matrix effect (Gross et al., 2000;Pratt and Prather, 2012). Thus, the particle counts and size distributions presented in this work should be interpreted as semi-quantitative and serve as a basis of comparison

analysis (Healy et al., 2012). Based on previous studies using ATOFMS and SPAMS instruments (Angelino et al., 2001;Huang et al., 2012;Zhang et al., 2012;Zauscher et al., 2013;Healy et al., 2015), amine-containing particles were characterized by marker ions, including *m/z* $^{59}(CH_3)_3N^+$, $^{74}(C_2H_5)_2NH_2^+$, $^{86}(C_2H_5)_2NCH_2^+$, $^{101}(C_2H_5)_3N^+$, $^{102}(C_3H_7)_2NH_2^+$, and $^{143}(C_3H_7)_3N^+$ (Table 1). In this work, a particle was identified as amine-containing if it contained any of the marker ions listed above with a relative peak area (defined as the percentage contribution of the target ion peak area to the sum of all ion peak areas) greater than 1%. It should be noted that amine-containing particles are operationally defined and not exclusive, which also contained various chemical species in addition to amines. According to this criterion, 57452 and 68026 amine-containing particles were identified in summer and winter, respectively, which accounted for 11.1 % and 9.4 % of the total detected particles. These number fractions are consistent with previously reported observations in the PRD (Zhang et al., 2012). However, due to the absence of fog events during the campaign, no dramatic increases in amine-containing particles associated with high RH conditions (RH > 90 %) were observed. Marker ions of $^{59}(CH_3)_3N^+$, $^{74}(C_2H_5)_2NH_2^+$, $^{86}(C_2H_5)_2NCH_2^+$ were detected as the most abundant amines species during the sampling period, so particles containing each marker ion were selected to investigate the possible sources and characteristics of amine-containing particles. $^{30}CH_3NH^+$ is also an amine marker which has been reported by other single particle studies (Phares et al., 2003;Glagolenko and Phares, 2004). In this work the peak intensity of $^{30}CH_3NH^+$ was much lower compared with other amine markers, and all the particles containing $^{30}CH_3NH^+$ had strong signal of $^{74}(C_2H_5)_2NH_2^+$, so the $^{30}CH_3NH^+$-containing particles were not specifically discussed. Ion of m/z +46 was detected in the ambient single particles, which could be the amine marker of $^{46}(CH_3)_2NH_2^+$ and/or $^{46}Na_2^+$ according to reported studies (Guazzotti et al., 2001;Gaston et al., 2011;Healy et al., 2015). In this work the m/z +46-containing particles had no other amine markers as listed above, besides, these particles were enriched with sodium salts like $^{62}Na_2O^+$, $^{81}Na_2Cl^+$ and $^{147}Na(NO_3)_2^-$. Thus, m/z +46-containing particles were not classified as amine-containing particles.

# 3 Results and Discussion

## 3.1 Seasonal variation of amine-containing particles

Spatial distributions of amine-containing particles associated with backward trajectories (48 hour) of air masses at 500m levels above the ground during the sampling period are shown in Figure 1. Cluster trajectories were calculated by MeteoInfo (Wang, 2014), and the box plots were conducted by Igor Pro-based program Histbox (Wu et al., 2018;Wu and Yu, 2018). In summer, high amine-containing particle counts were associated with air masses of Cluster 3 (41.67%) and Cluster 4 (30.06%) (Figure 1a) from continent and South China Sea separately, suggesting that the majority of amine-containing particles came from anthropogenic and marine sources. However, in winter, large amounts of amine-containing particles were associated with air masses of Cluster 4 (48.08%) (Figure 1b), indicating that amine-containing particles were related primarily with local emissions, such as animal husbandry, biomass burning, and vehicle exhaust. Anthropogenic emissions from Foshan and Guangzhou may also have contributed, as the sampling site is only 40 km and 56 km from these cities, respectively (Figure S1).

The amine-containing particle count observed in summer (57452) was lower than it observed in winter (68026), but the abundance of amine-containing particles relative to the total particle count was higher in summer (11.1%) than in winter (9.4%). Temporal variations of total amine-containing particles and three amine marker ions are shown in Figure 2. The increase of amine-containing particles was mostly associated with high relative humidity (RH) at night in summer, while no direct connection between particle counts and RH was found in winter (Figure S2 a and b). High counts of amine-containing particles that extended in a few days were found from 22 to 24 July (in summer) and from 5 to 8 February (in winter). Among the three markers we considered, the most abundant amine marker was $^{74}(C_2H_5)_2NH_2^+$, which was detected in 90% and 86% of amine-containing particles in summer and winter (Table 2), followed by $^{59}(CH_3)_3N^+$ and $^{86}(C_2H_5)_2NCH_2^+$ which were detected in less than 10% of amine-containing particles during sampling period. The amine particles

containing $^{74}(C_2H_5)_2NH_2^+$ and $^{86}(C_2H_5)_2NCH_2^+$ both exhibited similar variation pattern with total amine-containing particles suggesting a similar emission source of $^{74}(C_2H_5)_2NH_2^+$ and $^{86}(C_2H_5)_2NCH_2^+$ (Figure 2). The temporal trend of $^{59}(CH_3)_3N^+$-containing particles were different from those of $^{74}(C_2H_5)_2NH_2^+$ and $^{86}(C_2H_5)_2NCH_2^+$; and the two sudden episodes of $^{59}(CH_3)_3N^+$ occurred from 27 to 29 July in summer were possibly due to the special emission sources of trimethylamine (TMA).

The diurnal patterns of amine-containing particles are investigated in summer and winter (Figure 3) and both showed higher count at night. The small increase from 6:00 to 9:00 LST throughout the campaign may have been due to local emissions from vehicle exhaust (Cadle and Mulawa, 1980). Several field studies have revealed the strong correlation between RH and particulate amines, suggesting that high RH in fog events is favorable for the gas-to-particle partitioning of amines (Jeong et al., 2011;Rehbein et al., 2011;Huang et al., 2012;Zhang et al., 2012). In this work, although the increase of amine-containing particle count mostly occurred at night, no obvious correlations between diurnal amine-containing particles and RH were found in summer ($r^2$=0.33) and winter ($r^2$=0.0003) (Figure S2). The increase of amine-containing particles at night may be influenced by particle acidity and emission sources of amines (Murphy et al., 2007;Kurten et al., 2008;Silva et al., 2008).

**3.2 Characteristics of amine-containing particles**

The average mass spectra of amine-containing particles in summer and winter are shown in Figure 4. The amine-containing particles were characterized by high fractions of carbonaceous marker ions, including $^{27}C_2H_3^+$, $^{29}C_2H_5^+$, $^{36}C_3^+$, $^{37}C_3H^+$, $^{43}C_2H_3O^+$, $^{48}C_4^+$, $^{51}C_4H_3^+$, $^{53}C_4H_5^+$, $^{60}C_5^+$, $^{63}C_5H_3^+$, $^{65}C_5H_5^+$, and $^{77}C_6H_5^+$; and amine marker ions of $^{30}CH_3NH^+$, $^{59}(CH_3)_3N^+$, $^{74}(C_2H_5)_2NH_2^+$ and $^{86}(C_2H_5)_2NCH_2^+$ in the positive mass spectrum in both summer and winter. The negative mass spectrum was characterized by strong carbon-nitrogen fragments like $^{26}CN^-$ and $^{42}CNO^-$, as well as abundant secondary ions of $^{46}NO_2^-$, $^{62}NO_3^-$, $^{80}SO_3^-$, and $^{97}HSO_4^-$ in both summer and winter. In many field studies, aged carbonaceous particles always contain abundant secondary ions of sulfate, nitrate, and ammonium. Interestingly, in this work, the

signals of $^{18}NH_4^+$ were weak and only observed in less than 10% of amine-containing particles in summer, but moderate signal of $^{18}NH_4^+$ was detected in half of amine-containing particles in winter. The low $^{18}NH_4^+$ signal in amine-containing particles may have been due to the emission sources of ammonia and particle acidity, which will be discussed in Section 3.3.

The unscaled size-resolved number distributions of total amine-containing particles and amine particles containing three marker ions of $^{59}(CH_3)_3N^+$, $^{74}(C_2H_5)_2NH_2^+$, and $^{86}(C_2H_5)_2NCH_2^+$ are shown in Figure 5. The amine-containing particles exhibited unimodal distributions in the submicron mode from 0.4 to 1.5 μm in both summer and winter, which may have resulted from gaseous amine condensation on and/or reaction with fine mode particles from anthropogenic emissions. Although amine-containing particles peaked at the size range of 0.5-0.7 μm in both summer and winter, a broader size range of amine-containing particles was observed in winter, which may be due to more complex anthropogenic emission sources of primary particles in winter. The $^{74}(C_2H_5)_2NH_2^+$-containing particles showed similar variation patterns as total amine-containing particles both in summer and winter. However, $^{59}(CH_3)_3N^+$- and $^{86}(C_2H_5)_2NCH_2^+$-containing particles showed less distinct peaks in winter.

**3.3 Mixing state and formation processes of amine-containing particles**

To investigate the aging state of amine-containing particles, the abundances of sulfate-, nitrate-, and ammonium-containing amine particles are shown in Table 3. More than 90% of amine-containing particles were found to be internally mixed with sulfate throughout the sampling period. The abundance of nitrate in amine particles increased from 43% in summer to 69% in winter. The high abundances of sulfate and nitrate in amine-containing particles suggest the possible formation of aminium sulfate and nitrate salts. Interestingly, only 8% of amine-containing particles mixed with ammonium ($NH_4^+$) in summer, while the percentage increased dramatically to 54 % in winter, indicating a relatively $NH_4^+$-poor state in summer and an $NH_4^+$-rich state in winter.

The seasonal differences of the mixing state of amines and $NH_4^+$ may be

influenced by the seasonal variation of source strength of $NH_4^+$. To investigate the temporal variation and abundance of $NH_4^+$ in total detected single particles, the total $NH_4^+$-containing particles were identified with relative area of $^{18}NH_4^+$ larger than 1%. Using this criterion, 18336 and 235312 of $NH_4^+$-containing particles were detected in summer and winter separately, accounting for 3.6% and 32.6% of the total detected particles. The averaged positive and negative ion mass spectra of $NH_4^+$-containing particles are exhibited in Figure 6. During entire sampling period the $NH_4^+$-containing particles were characterized by abundant hydrocarbon fragments and secondary organic species like $^{43}C_2H_3O^+$ and $^{89}HC_2O_4^-$, as well as strong signals of $^{26}CN^-$, $^{42}CNO^-$, $^{62}NO_3^-$ and $^{97}HSO_4^-$, indicating an aging state of $NH_4^+$-containing particles. Also, 20% of $NH_4^+$-containing particles contained $^{74}(C_2H_5)_2NH_2^+$, which indicates a close connection between $NH_3$ and diethylamine (DEA), possibly due to the similar emission sources.

Temporal variations of total amine-containing particles, total ammonium-containing ($NH_4^+$-containing) particles and particles containing both ammonium and amine ($NH_4^+$-amine) are shown in Figure 7. The total $NH_4^+$-containing particles and $NH_4^+$-amine particles were both much lower in summer than in winter. This seasonal difference may be due to the low emission sources of ammonia and preferred partitioning in gas phase in summer. Backward trajectories analysis (Figure 1) showed that in summer the air mass was mainly from south of the sampling site and linked to the marine region with low emission of anthropogenic pollutants. By contrast, in winter, the air mass was mainly from northwest of the sampling site and associated with relatively polluted megacities like Guangzhou and Foshan. RH does not seem to exert a major influence on particulate $NH_4^+$ (Huang et al., 2012), because lower abundance of $NH_4^+$ was observed in summer (RH = 72 ± 13%) than in winter (RH =63 ± 11%).

The temporal variations of the peak areas of amines, ammonium, and the sum of sulfate and nitrate in amine-containing particles are shown in Figure 8. The peak areas of amines and the sum of nitrate and sulfate had similar variation patterns both in summer and winter. The linear regression between them showed robust correlations

both in summer ($r^2$=0.74) and winter ($r^2$=0.88) (Figure S3), indicating the formation of aminium salts. Low peak area of ammonium was found in the amine-containing particles in summer which was in accordance with the small amount of $NH_4^+$-amine particles. However, in winter, the peak area of ammonium was comparable with amines and they both exhibited similar temporal trends. The sum of the sulfate and nitrate peak areas had a higher increase rate than the amine peak area from 6 to 8 February, which may have been caused by an increase of ammonium during this period. In this work the particle acidity of amine-containing particles is represented by the relative acidity ratio ($R_a$), which is defined as the ratio of the sum of the sulfate and nitrate peak areas divided by the ammonium peak area (Denkenberger et al., 2007;Pratt et al., 2009;Cheng et al., 2017). Huang et al. (2013) obtained a robust correlation ($r^2$=0.82) between the particle acidity calculated from inorganic ions obtained from MARGA and relative acidity ratio obtained from single particle mass spectrometer, allowing us to use $R_a$ for comparison of particle acidity(Huang et al., 2013). The $R_a$ was 326 $\pm$ 326 in summer and 31 $\pm$ 13 in winter (Figure 8), indicating that the amine-containing particles were more acidic in summer than in winter.

Although high acidity promotes gaseous ammonia partitioning, extremely low ammonium peak areas were found for the amine-containing particles in summer (Figure 8), which may be associated with ammonium–amine exchange reactions in addition to the low emission source of ammonia. The exchange between amine gases and particulate $NH_3$ and/or ammonium highly depends on the RH and particle acidity (Chan and Chan, 2013;Chu and Chan, 2016). According to the study of Sauerwein and Chan, the co-uptake of dimethylamine (DMA) and ammonia ($NH_3$) by sulfuric acid particles at 50% RH led to particle-phase dimethylaminium ($DMAH^+$) to ammonium ($NH_4^+$) molar ratio up to four times that of gas-phase DMA to ammonia molar ratio (0.1 and 0.5), suggesting the displacement of $NH_4^+$ by DMA during the uptake process (Sauerwein and Chan, 2017). In this work, the ambient RH and acidic particles containing abundant sulfate and nitrate were similar to the experimental conditions used in Sauerwein and Chan (2017). In summer 8% of amine-containing particles contained $NH_4^+$, while 25% of ammonium-containing particles contained

amines (Figure 7). Although the gas-phase concentrations of amines and $NH_3$ are not quantified, higher abundance of amines in ammonium-containing particles than that of ammonium in amine-containing particles suggests a possible ammonium–amine exchange reactions in acidic particles in summer.

As strong bases, the presence of amines could have an impact on the particle acidity. After including amines along with the ammonium in the relative acidity ratio calculation, the new $R_a'$ values (redefined as the ratio of the sum of the sulfate and nitrate peak areas to the sum of the ammonium and amine peak areas) decrease to 11 $\pm$ 4 and 10 $\pm$ 2 in summer and winter, respectively, which are 30 and 3 times lower than $R_a$ values. Besides, $R_a'$ showed no obvious seasonal change of particle acidity, which suggests that amines could be a buffer for the particle acidity of ammonium-poor particles, implying that it is reasonable to consider amines to calculate particle acidity and actual pH. In addition, the presence of aminium salts affects the water activities and osmotic coefficients of aqueous solutions, which may influence the calculation of pH using aerosol thermodynamic models (Sauerwein et al., 2015). Furthermore, it should be noted that the measured pH of bulk ambient aerosols may not be representative of the actual single particle acidity. Hence, the mixing state of aerosols should be considered in order to comprehensively estimate the aerosol pH (Pratt et al., 2009). Several recent studies have reported a ‘missing’ source of sulfate produced from the oxidation of $SO_2$ by $NO_2$ during haze episodes with high ambient relative humidity in northern China, and the neutralization of particulate ammonium is a key factor in this formation mechanism (Cheng et al., 2016;Wang et al., 2016). Our study reveals that amines have a potential influence on particle acidity, which could also impact this sulfate formation process during haze episodes. In order to discuss the potential role of amines in this sulfate formation pathway, real-time concentrations of amines, ammonium, sulfate, nitrate, and their precursors must be available. The results of this study suggest that amine chemistry involving particle acidity and mixing state with sulfate, nitrate and ammonium may have an important role in the aging process of particles in regions with high concentration of amines.

## 4 Summary and Conclusions

Amine-containing particles were investigated using a single particle aerosol mass spectrometer from 18 July to 1 August 2014, and from 27 January to 8 February 2015 in Heshan, China. Amine-containing particles accounted for 11.1 % and 9.4 % of the total detected single particles in summer and winter, respectively; both seasons were dominated by amine marker of $^{74}(C_2H_5)_2NH_2^+$ in 90% and 86% of amine-containing particles in summer and winter, respectively. Amine markers of $^{59}(CH_3)_3N^+$ and $^{86}(C_2H_5)_2NCH_2^+$ were detected in 4.5% and 5.5% of amine-containing particles in summer, while their percentages both increased two times in winter. The amine particles contained $^{74}(C_2H_5)_2NH_2^+$ and $^{86}(C_2H_5)_2NCH_2^+$ both exhibited similar variation pattern with total amine-containing particles suggesting a similar emission source of $^{74}(C_2H_5)_2NH_2^+$ and $^{86}(C_2H_5)_2NCH_2^+$, while the $^{59}(CH_3)_3N^+$-containing particles showed different temporal trends, and two sudden increase episodes of $^{59}(CH_3)_3N^+$ in summer was possibly due to the special sources of trimethylamine. Although the increase of amine-containing particle count mostly occurred at night, no obvious correlations between amine-containing particles and RH were found in summer ($r^2$=0.33) and winter ($r^2$=0.0003). More than 90% of amine-containing particles contained strong signals of sulfate throughout the sampling period, while 43% and 69% of amine particles contained nitrate in summer in winter. Robust correlations between the peak intensities of amines and the sum of nitrate and sulfate suggested the possible formation of aminium sulfate and nitrate salts. Only 8% of amine particles contained ammonium in summer, while the percentage increased dramatically to 54% in winter. Due to the lower percentage of total ammonium-containing particles in summer (3.6%) than it in winter (32.6%), the relatively ammonium-poor state of amine-containing particles in summer may be due to the lower abundance of ammonia/ammonium in gas and particle phase. Besides, 8% of amine-containing particles contained ammonium while 25% of ammonium-containing particles contained amines in summer, suggesting a possible contribution of ammonium–amine exchange reactions to the low abundance of

ammonium in amine-containing particles at high ambient RH (72 ± 13 %) in summer. In order to estimate the particle acidity, the relative acidity ratio ($R_a$), defined as the ratio of the sum of the sulfate and nitrate peak areas divided by the ammonium peak area, was calculated and showed higher values in summer (326 ± 326) than (31 ± 13) in winter, suggesting the amine-containing particles were more acidic in summer than in winter. However, after including amines along with the ammonium in the acidity calculation, the new $R_a$' values showed no distinct seasonal change (summer: 11 ± 4; winter: 10 ± 2), suggesting that it is reasonable to consider amines when estimating particle acidity.

**Author contributions:** Chunlei Cheng and Mei Li designed the experiments. Tao Zhang, Yubo Ou and Duohong Chen carried them out. Chunlei Cheng prepared the manuscript with contributions from all co-authors.

**Competing interests:** Bo Huang and Zhong Fu are both employees at Guangzhou Hexin Analytical Instrument Limited Company.

***Acknowledgements***: This work was financially supported by the NSFC of Guangdong Province (Grant Nos. 2017A030310180, 2015A030313339), National Natural Science Foundation of China (Grant No.21607056), National Key Technology R&D Program (Grant No. 2014BAC21B01), Guangdong Province Public Interest Research and Capacity Building Special Fund (Grant No. 2014B020216005), the Guangdong Applied Science and Technology Research and Development (Grant No. 2015B020236003), Fundamental Research Funds for the Central Universities (Grant No. 21617455), National research program for key issues in air pollution control (Grant No. DQGG0107), National Key Research and Development Program of China (Grant No. 2016YFC0208503), and Pearl River Nova Program of Guangzhou (No. 201506010013). Chak K. Chan would like to acknowledge funding support from the General Fund of National Natural Science Foundation of China (Grant No. 41675117).

The authors acknowledge sampling support from the Guangdong Atmospheric Supersite. Helpful comments and revisions from Anthony S. Wexler, Hang Su and Misha I.S. Boehm are acknowledged as well.

## References

Angelino, S., Suess, D. T., and Prather, K. A.: Formation of aerosol particles from reactions of secondary and tertiary alkylamines: Characterization by aerosol time-of-flight mass spectrometry, Environmental Science & Technology, 35, 3130-3138, Doi 10.1021/Es0015444, 2001.

Berndt, T., Stratmann, F., Sipila, M., Vanhanen, J., Petaja, T., Mikkila, J., Gruner, A., Spindler, G., Mauldin, R. L., Curtius, J., Kulmala, M., and Heintzenberg, J.: Laboratory study on new particle formation from the reaction OH + SO2: influence of experimental conditions, H2O vapour, NH3 and the amine tert-butylamine on the overall process, Atmospheric Chemistry and Physics, 10, 7101-7116, 10.5194/acp-10-7101-2010, 2010.

Bzdek, B., Ridge, D., and Johnston, M.: Amine exchange into ammonium bisulfate and ammonium nitrate nuclei, Atmospheric Chemistry and Physics, 10, 3495-3503, 2010.

Cadle, S. H., and Mulawa, P. A.: Low-molecular-weight aliphatic amines in exhaust from catalyst-equipped cars, Environmental science & technology, 14, 718-723, 1980.

Calderon, S. M., Poor, N. D., and Campbell, S. W.: Estimation of the particle and gas scavenging contributions to wet deposition of organic nitrogen, Atmospheric Environment, 41, 4281-4290, 10.1016/j.atmosenv.2006.06.067, 2007.

Chan, L. P., and Chan, C. K.: Role of the Aerosol Phase State in Ammonia/Amines Exchange Reactions, Environmental Science & Technology, 47, 5755-5762, 10.1021/es4004685, 2013.

Cheng, C., Li, M., Chan, C. K., Tong, H., Chen, C., Chen, D., Wu, D., Li, L., Wu, C., Cheng, P., Gao, W., Huang, Z., Li, X., Zhang, Z., Fu, Z., Bi, Y., and Zhou, Z.: Mixing state of oxalic acid containing particles in the rural area of Pearl River Delta, China: implications for the formation mechanism of oxalic acid, Atmospheric Chemistry and Physics, 17, 9519-9533, 10.5194/acp-17-9519-2017, 2017.

Cheng, Y., Zheng, G., Wei, C., Mu, Q., Zheng, B., Wang, Z., Gao, M., Zhang, Q., He, K., Carmichael, G., Pöschl, U., and Su, H.: Reactive nitrogen chemistry in aerosol water as a source of sulfate during haze events in China, Science Advances, 2, 10.1126/sciadv.1601530, 2016.

Chu, Y., and Chan, C. K.: Reactive Uptake of Dimethylamine by Ammonium Sulfate and Ammonium Sulfate–Sucrose Mixed Particles, The Journal of Physical Chemistry A, 121, 206-215, 10.1021/acs.jpca.6b10692, 2016.

Chu, Y., and Chan, C. K.: Role of oleic acid coating in the heterogeneous uptake of dimethylamine by ammonium sulfate particles, Aerosol Science and Technology, 51, 988-997, 10.1080/02786826.2017.1323072, 2017.

Chu, Y. X., Sauerwein, M., and Chan, C. K.: Hygroscopic and phase transition properties of alkyl aminium sulfates at low relative humidities, Phys Chem Chem Phys, 17, 19789-19796, 10.1039/c5cp02404h, 2015.

Day, D. A., Takahama, S., Gilardoni, S., and Russell, L. M.: Organic composition of single and submicron particles in different regions of western North America and the eastern Pacific during INTEX-B 2006, Atmospheric Chemistry and Physics, 9, 5433-5446, 2009.

Denkenberger, K. A., Moffet, R. C., Holecek, J. C., Rebotier, T. P., and Prather, K. A.: Real-time, single-particle measurements of oligomers in aged ambient aerosol particles, Environmental Science & Technology, 41, 5439-5446, 10.1021/es070329l, 2007.

Gaston, C. J., Furutani, H., Guazzotti, S. A., Coffee, K. R., Bates, T. S., Quinn, P. K., Aluwihare, L. I., Mitchell, B. G., and Prather, K. A.: Unique ocean‐derived particles serve as a proxy for changes in ocean chemistry, Journal of Geophysical Research: Atmospheres (1984–2012), 116, 10.1029/2010JD015289, 2011.

Ge, X. L., Wexler, A. S., and Clegg, S. L.: Atmospheric amines - Part II. Thermodynamic properties and gas/particle partitioning, Atmospheric Environment, 45, 561-577, 10.1016/j.atmosenv.2010.10.013, 2011a.

Ge, X. L., Wexler, A. S., and Clegg, S. L.: Atmospheric amines - Part I. A review, Atmospheric Environment, 45, 524-546, DOI 10.1016/j.atmosenv.2010.10.012, 2011b.

Gilardoni, S., Liu, S., Takahama, S., Russell, L. M., Allan, J. D., Steinbrecher, R., Jimenez, J. L., De Carlo, P. F., Dunlea, E. J., and Baumgardner, D.: Characterization of organic ambient aerosol during MIRAGE 2006 on three platforms, Atmospheric Chemistry and Physics, 9, 5417-5432, 2009.

Glagolenko, S., and Phares, D. J.: Single-particle analysis of ultrafine aerosol in College Station, Texas, Journal of Geophysical Research-Atmospheres, 109, 10.1029/2004jd004621, 2004.

Gross, D. S., Galli, M. E., Silva, P. J., and Prather, K. A.: Relative sensitivity factors for alkali metal and ammonium cations in single particle aerosol time-of-flight mass spectra, Anal. Chem., 72, 416-422, Doi 10.1021/Ac990434g, 2000.

Guazzotti, S. A., Whiteaker, J. R., Suess, D., Coffee, K. R., and Prather, K. A.: Real-time measurements of the chemical composition of size-resolved particles during a Santa Ana wind episode, California USA, Atmospheric Environment, 35, 3229-3240, 2001.

Healy, R., Sciare, J., Poulain, L., Kamili, K., Merkel, M., Müller, T., Wiedensohler, A., Eckhardt, S., Stohl, A., and Sarda-Estève, R.: Sources and mixing state of size-resolved elemental carbon particles in a European megacity: Paris, Atmospheric Chemistry and Physics, 12, 1681-1700, 2012.

Healy, R. M., Evans, G. J., Murphy, M., Sierau, B., Arndt, J., McGillicuddy, E., O'Connor, I. P., Sodeau, J. R., and Wenger, J. C.: Single-particle speciation of

alkylamines in ambient aerosol at five European sites, Analytical and Bioanalytical Chemistry, 407, 5899-5909, 10.1007/s00216-014-8092-1, 2015.
Huang, Y., Chen, H., Wang, L., Yang, X., and Chen, J.: Single particle analysis of amines in ambient aerosol in Shanghai, Environmental Chemistry, 9, 202-210, 10.1071/EN11145, 2012.
Huang, Y., Li, L., Li, J., Wang, X., Chen, H., Chen, J., Yang, X., Gross, D. S., Wang, H., Qiao, L., and Chen, C.: A case study of the highly time-resolved evolution of aerosol chemical and optical properties in urban Shanghai, China, Atmospheric Chemistry and Physics, 13, 3931-3944, 10.5194/acp-13-3931-2013, 2013.
Jeong, C. H., McGuire, M. L., Godri, K. J., Slowik, J. G., Rehbein, P. J. G., and Evans, G. J.: Quantification of aerosol chemical composition using continuous single particle measurements, Atmospheric Chemistry and Physics, 11, 7027-7044, 10.5194/acp-11-7027-2011, 2011.
Kurten, T., Loukonen, V., Vehkamaki, H., and Kulmala, M.: Amines are likely to enhance neutral and ion-induced sulfuric acid-water nucleation in the atmosphere more effectively than ammonia, Atmospheric Chemistry and Physics, 8, 4095-4103, 2008.
Lee, D., and Wexler, A. S.: Atmospheric amines - Part III: Photochemistry and toxicity, Atmospheric Environment, 71, 95-103, DOI 10.1016/j.atmosenv.2013.01.058, 2013.
Li, L., Huang, Z. X., Dong, J. G., Li, M., Gao, W., Nian, H. Q., Fu, Z., Zhang, G. H., Bi, X. H., Cheng, P., and Zhou, Z.: Real time bipolar time-of-flight mass spectrometer for analyzing single aerosol particles, Int J Mass Spectrom, 303, 118-124, 10.1016/j.ijms.2011.01.017, 2011.
Liu, S., Takahama, S., Russell, L. M., Gilardoni, S., and Baumgardner, D.: Oxygenated organic functional groups and their sources in single and submicron organic particles in MILAGRO 2006 campaign, Atmospheric Chemistry and Physics, 9, 6849-6863, 2009.
Liu, Y., Han, C., Liu, C., Ma, J., Ma, Q., and He, H.: Differences in the reactivity of ammonium salts with methylamine, Atmospheric Chemistry and Physics, 12, 4855-4865, 2012.
Lloyd, J. A., Heaton, K. J., and Johnston, M. V.: Reactive uptake of trimethylamine into ammonium nitrate particles, The Journal of Physical Chemistry A, 113, 4840-4843, 10.1021/jp900634d, 2009.
Malloy, Q. G. J., Li, Q., Warren, B., Cocker Iii, D. R., Erupe, M. E., and Silva, P. J.: Secondary organic aerosol formation from primary aliphatic amines with NO<sub>3</sub> radical, Atmos. Chem. Phys., 9, 2051-2060, 10.5194/acp-9-2051-2009, 2009.
Moffet, R. C., de Foy, B., Molina, L. T., Molina, M. J., and Prather, K. A.: Measurement of ambient aerosols in northern Mexico City by single particle mass spectrometry, Atmospheric Chemistry and Physics, 8, 4499-4516, 10.5194/acp-8-4499-2008, 2008.
Murphy, S. M., Sorooshian, A., Kroll, J. H., Ng, N. L., Chhabra, P., Tong, C., Surratt, J. D., Knipping, E., Flagan, R. C., and Seinfeld, J. H.: Secondary aerosol

585 formation from atmospheric reactions of aliphatic amines, Atmospheric
586 Chemistry and Physics, 7, 2313-2337, 2007.
587 Ngwabie, N. M., Schade, G. W., Custer, T. G., Linke, S., and Hinz, T.: Volatile organic
588 compound emission and other trace gases from selected animal buildings,
589 Landbauforsch Volk, 57, 273-284, 2007.
590 Noble, C. A., and Prather, K. A.: Real-time measurement of correlated size and
591 composition profiles of individual atmospheric aerosol particles, Environmental
592 science & technology, 30, 2667-2680, 1996.
593 Phares, D. J., Rhoads, K. P., Johnston, M. V., and Wexler, A. S.: Size-resolved
594 ultrafine particle composition analysis - 2. Houston, Journal of Geophysical
595 Research-Atmospheres, 108, 10.1029/2001jd001212, 2003.
596 Place, P. F., Ziemba, L. D., and Griffin, R. J.: Observations of nucleation-mode
597 particle events and size distributions at a rural New England site, Atmospheric
598 Environment, 44, 88-94, 10.1016/j.atmosenv.2009.09.030, 2010.
599 Prather, K. A., Nordmeyer, T., and Salt, K.: Real-time characterization of individual
600 aerosol particles using time-of-flight mass spectrometry, Anal. Chem., 66,
601 1403-1407, 1994.
602 Pratt, K. A., Hatch, L. E., and Prather, K. A.: Seasonal Volatility Dependence of
603 Ambient Particle Phase Amines, Environmental Science & Technology, 43,
604 5276-5281, 10.1021/es803189n, 2009.
605 Pratt, K. A., and Prather, K. A.: Mass spectrometry of atmospheric aerosols—Recent
606 developments and applications. Part II: On‐line mass spectrometry techniques,
607 Mass Spectrom Rev, 31, 17-48, 2012.
608 Qiu, C., Wang, L., Lal, V., Khalizov, A. F., and Zhang, R.: Heterogeneous reactions of
609 alkylamines with ammonium sulfate and ammonium bisulfate, Environmental
610 science & technology, 45, 4748-4755, 2011.
611 Rappert, S., and Muller, R.: Odor compounds in waste gas emissions from agricultural
612 operations and food industries, Waste Manage, 25, 887-907,
613 10.1016/j.wasman.2005.07.008, 2005.
614 Rehbein, P. J. G., Jeong, C. H., McGuire, M. L., Yao, X. H., Corbin, J. C., and Evans,
615 G. J.: Cloud and Fog Processing Enhanced Gas-to-Particle Partitioning of
616 Trimethylamine, Environmental Science & Technology, 45, 4346-4352,
617 10.1021/es1042113, 2011.
618 Rogge, W. F., Hildemann, L. M., Mazurek, M. A., and Cass, G. R.: Sources of Fine
619 Organic Aerosol .6. Cigarette-Smoke in the Urban Atmosphere, Environmental
620 Science & Technology, 28, 1375-1388, 10.1021/Es00056a030, 1994.
621 Russell, L. M., Takahama, S., Liu, S., Hawkins, L. N., Covert, D. S., Quinn, P. K., and
622 Bates, T. S.: Oxygenated fraction and mass of organic aerosol from direct
623 emission and atmospheric processing measured on the R/V Ronald Brown during
624 TEXAQS/GoMACCS 2006, Journal of Geophysical Research-Atmospheres, 114,
625 10.1029/2008jd011275, 2009.
626 Sauerwein, M., Clegg, S. L., and Chan, C. K.: Water Activities and Osmotic
627 Coefficients of Aqueous Solutions of Five Alkylaminium Sulfates and Their
628 Mixtures with H2SO4 at 25(o)C, Aerosol Science and Technology, 49, 566-579,

10.1080/02786826.2015.1043045, 2015.
Sauerwein, M., and Chan, C. K.: Heterogeneous uptake of ammonia and dimethylamine into sulfuric and oxalic acid particles, Atmos. Chem. Phys., 17, 6323-6339, 10.5194/acp-17-6323-2017, 2017.
Silva, P. J., Erupe, M. E., Price, D., Elias, J., Malloy, Q. G. J., Li, Q., Warren, B., and Cocker, D. R.: Trimethylamine as precursor to secondary organic aerosol formation via nitrate radical reaction in the atmosphere, Environmental Science & Technology, 42, 4689-4696, Doi 10.1021/Es703016v, 2008.
Sorooshian, A., Ng, N. L., Chan, A. W. H., Feingold, G., Flagan, R. C., and Seinfeld, J. H.: Particulate organic acids and overall water-soluble aerosol composition measurements from the 2006 Gulf of Mexico Atmospheric Composition and Climate Study (GoMACCS), Journal of Geophysical Research-Atmospheres, 112, 10.1029/2007jd008537, 2007.
Sorooshian, A., Murphy, S. N., Hersey, S., Gates, H., Padro, L. T., Nenes, A., Brechtel, F. J., Jonsson, H., Flagan, R. C., and Seinfeld, J. H.: Comprehensive airborne characterization of aerosol from a major bovine source, Atmospheric Chemistry and Physics, 8, 5489-5520, 2008.
Wang, G., Zhang, R., Gomez, M. E., Yang, L., Levy Zamora, M., Hu, M., Lin, Y., Peng, J., Guo, S., Meng, J., Li, J., Cheng, C., Hu, T., Ren, Y., Wang, Y., Gao, J., Cao, J., An, Z., Zhou, W., Li, G., Wang, J., Tian, P., Marrero-Ortiz, W., Secrest, J., Du, Z., Zheng, J., Shang, D., Zeng, L., Shao, M., Wang, W., Huang, Y., Wang, Y., Zhu, Y., Li, Y., Hu, J., Pan, B., Cai, L., Cheng, Y., Ji, Y., Zhang, F., Rosenfeld, D., Liss, P. S., Duce, R. A., Kolb, C. E., and Molina, M. J.: Persistent sulfate formation from London Fog to Chinese haze, Proceedings of the National Academy of Sciences, 113, 13630-13635, 10.1073/pnas.1616540113, 2016.
Wang, L., Khalizov, A. F., Zheng, J., Xu, W., Ma, Y., Lal, V., and Zhang, R. Y.: Atmospheric nanoparticles formed from heterogeneous reactions of organics, Nat Geosci, 3, 238-242, 10.1038/NGEO778, 2010.
Wang, Y. Q.: MeteoInfo: GIS software for meteorological data visualization and analysis, Meteorol Appl, 21, 360-368, 10.1002/met.1345, 2014.
Williams, B. J., Goldstein, A. H., Kreisberg, N. M., Hering, S. V., Worsnop, D. R., Ulbrich, I. M., Docherty, K. S., and Jimenez, J. L.: Major components of atmospheric organic aerosol in southern California as determined by hourly measurements of source marker compounds, Atmospheric Chemistry and Physics, 10, 11577-11603, 10.5194/acp-10-11577-2010, 2010.
Wu, C., Wu, D., and Yu, J. Z.: Quantifying black carbon light absorption enhancement with a novel statistical approach, Atmospheric Chemistry and Physics, 18, 289-309, 10.5194/acp-18-289-2018, 2018.
Wu, C., and Yu, J. Z.: Evaluation of linear regression techniques for atmospheric applications: the importance of appropriate weighting, Atmos Meas Tech, 11, 1233-1250, 10.5194/amt-11-1233-2018, 2018.
Zauscher, M. D., Wang, Y., Moore, M. J. K., Gaston, C. J., and Prather, K. A.: Air Quality Impact and Physicochemical Aging of Biomass Burning Aerosols during the 2007 San Diego Wildfires, Environmental Science & Technology, 47,

7633-7643, 10.1021/es4004137, 2013.
Zhang, G., Bi, X., Chan, L. Y., Li, L., Wang, X., Feng, J., Sheng, G., Fu, J., Li, M., and Zhou, Z.: Enhanced trimethylamine-containing particles during fog events detected by single particle aerosol mass spectrometry in urban Guangzhou, China, Atmospheric Environment, 55, 121-126, 2012.

# Tables and Figures

## Table list:



## Figure captions:

relative acidity ratio ($R_a$), which was calculated as the ratio of the total sulfate and nitrate peak areas to the ammonium peak area, is plotted as log($R_a$).

## Tables:

Table 1. Marker ions chosen for the amine-containing particles

| Marker ion | Alkylamine assignment |
|---|---|
| $^{59}(CH_3)_3N^+$ | Trimethylamine (TMA) |
| $^{74}(C_2H_5)_2NH_2^+$ | Diethylamine (DEA) |
| $^{86}(C_2H_5)_2NCH_2^+$ | DEA, TEA, DPA |
| $^{101}(C_2H_5)_3N^+$ | Triethylamine (TEA) |
| $^{102}(C_3H_7)_2NH_2^+$ | Dipropylamine (DPA) |
| $^{143}(C_3H_7)_3N^+$ | Tripropylamine (TPA) |

Table 2. Seasonal distributions of amine-containing particles and three major amine markers in summer and winter in the PRD, China.

| | Summer (18/7-1/8, 2014) | | Winter (27/1-8/2, 2015) | |
|---|---|---|---|---|
| Particle type | Count | Percentage (%)[a] | Count | Percentage (%)[a] |
| Total Amines | 57452 | | 68026 | |
| $^{59}(CH_3)_3N^+$ | 2581 | 4.5 | 6894 | 10 |
| $^{74}(C_2H_5)_2NH_2^+$ | 51442 | 90 | 58272 | 86 |
| $^{86}(C_2H_5)_2NCH_2^+$ | 3185 | 5.5 | 6119 | 9 |

[a]The percentage of each amine marker ion in total detected amine-containing particles.

Table 3. The abundances of ammonium-, nitrate- and sulfate-containing amine particles in total amine-containing particles.

| Marker ions | Summer | Winter |
|---|---|---|
| $^{18}NH_4^+$ | 8% | 54% |
| $^{62}NO_3^-$ | 43% | 69% |
| $^{97}HSO_4^-$ | 91% | 94% |

The marker ions of $^{18}NH_4^+$, $^{62}NO_3^-$ and $^{97}HSO_4^-$ were chosen to represent ammonium, nitrate and sulfate.

## Figures:

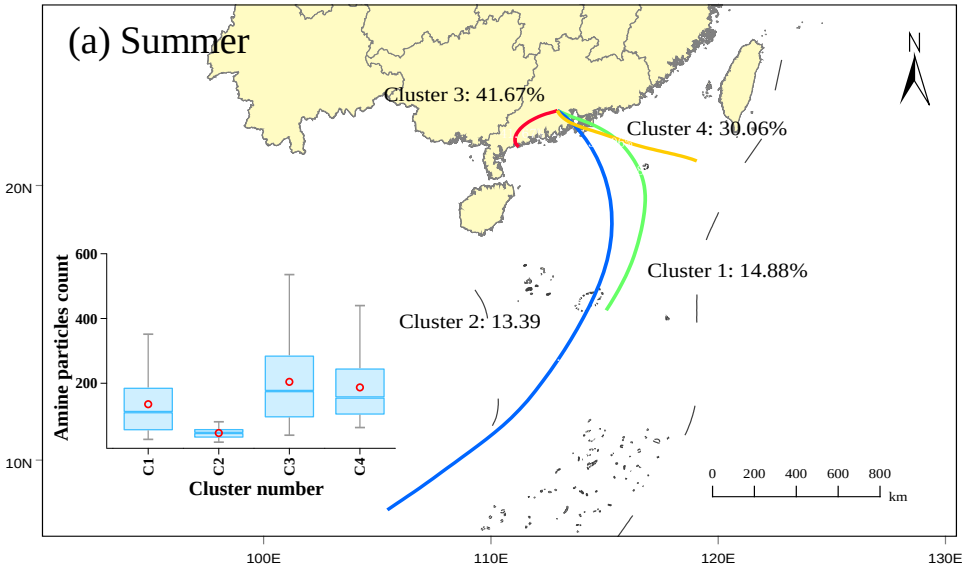


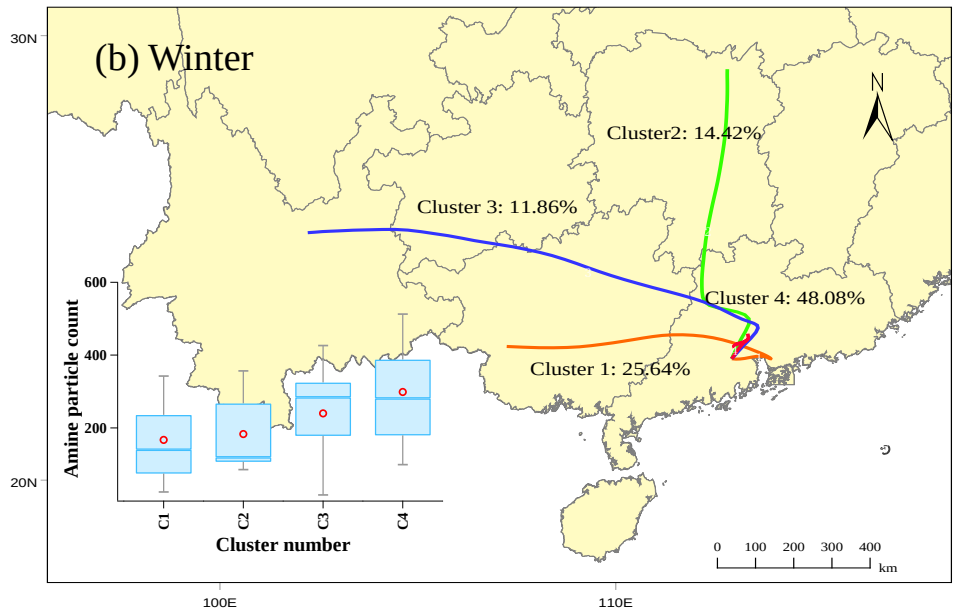


Figure 1. Spatial distributions of amine-containing particle counts associated with backward trajectories (48 hour) of air masses at 500m levels above the ground during the sampling period: (a) summer (from July 18 to August 1, 2014), (b) winter (from January 27 to February 8, 2015).

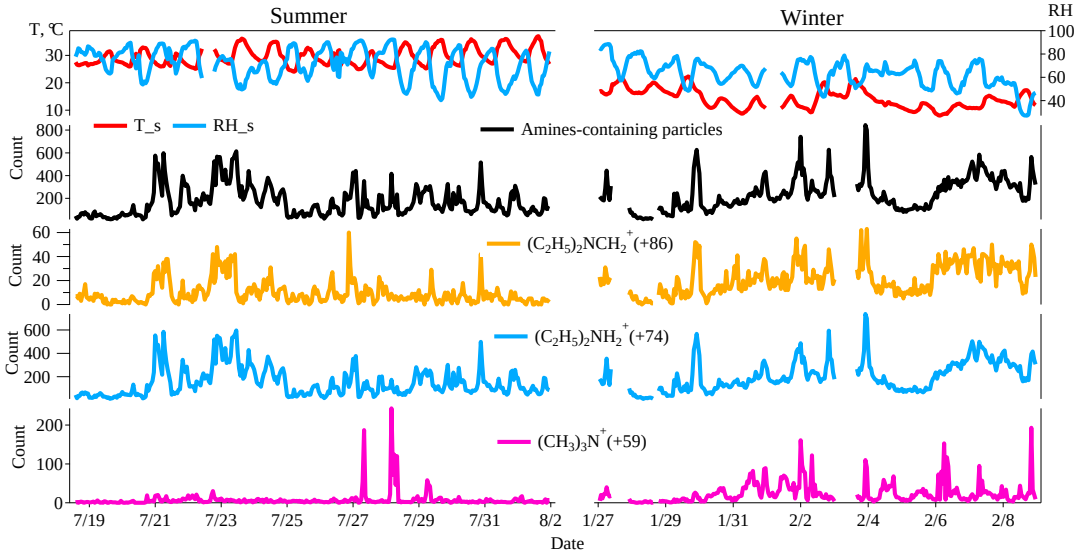


Figure 2. Temporal variations of relative humidity (RH), temperature (T), total amine-containing particles, and three major marker ions-containing amine particles ($^{59}(CH_3)_3N^+$, $^{74}(C_2H_5)_2NH_2^+$, $^{86}(C_2H_5)_2NCH_2^+$) in Heshan, China during sampling periods.

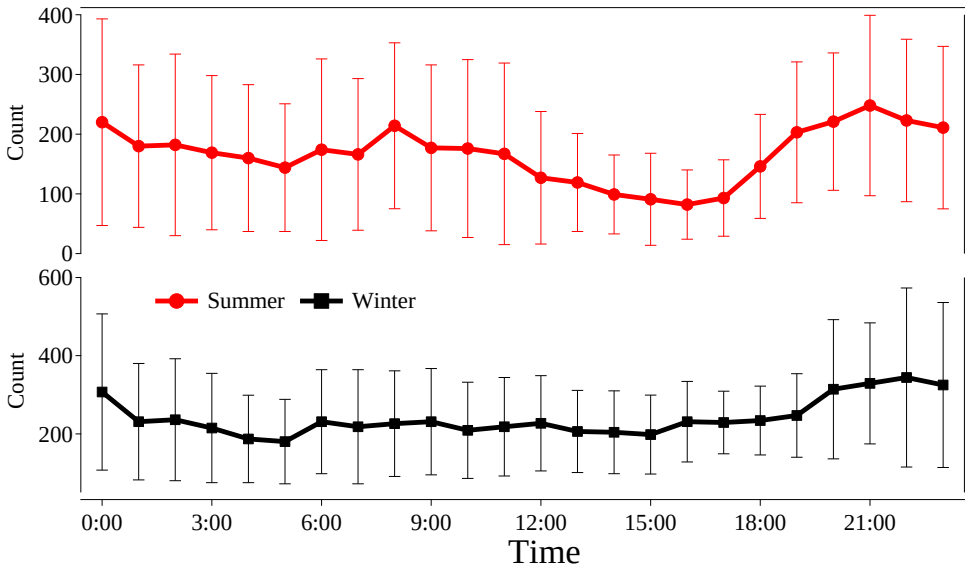


Figure 3. Diurnal variations of amine-containing particle counts in summer and winter in Heshan.

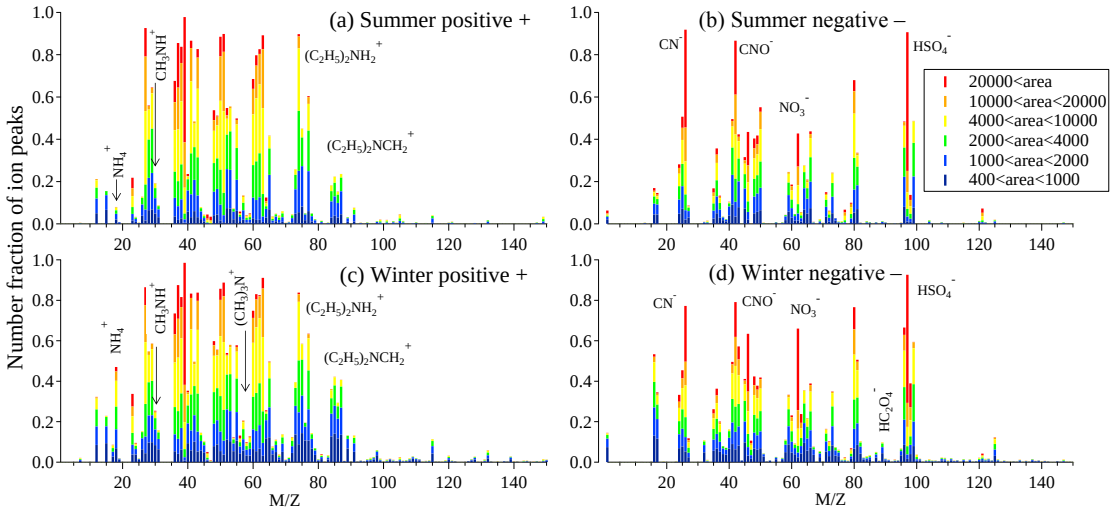


Figure 4. Average ion mass spectra of amine-containing particles in summer and winter. The color bars represent each peak area corresponding to a specific ion in individual particles.

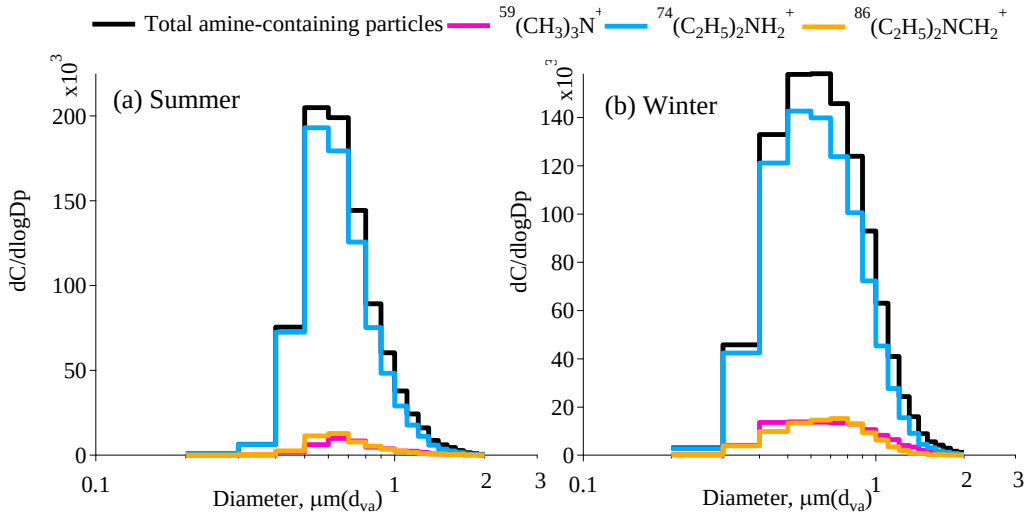


Figure 5. Unscaled size-resolved number distributions of total amine-containing particles and amine particles containing three marker ions of $^{59}(CH_3)_3N^+$, $^{74}(C_2H_5)_2NH_2^+$, and $^{86}(C_2H_5)_2NCH_2^+$ in summer and winter in Heshan.

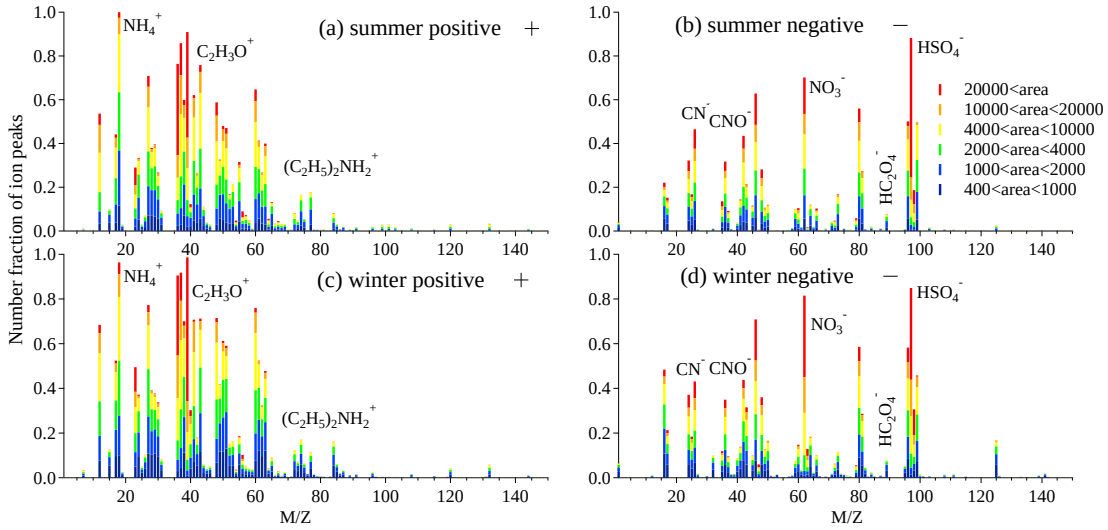


Figure 6. Mass spectra of total ammonium-containing ($NH_4^+$-containing) particles in summer and winter. The color bars represent each peak area corresponding to a specific fraction in individual particles.

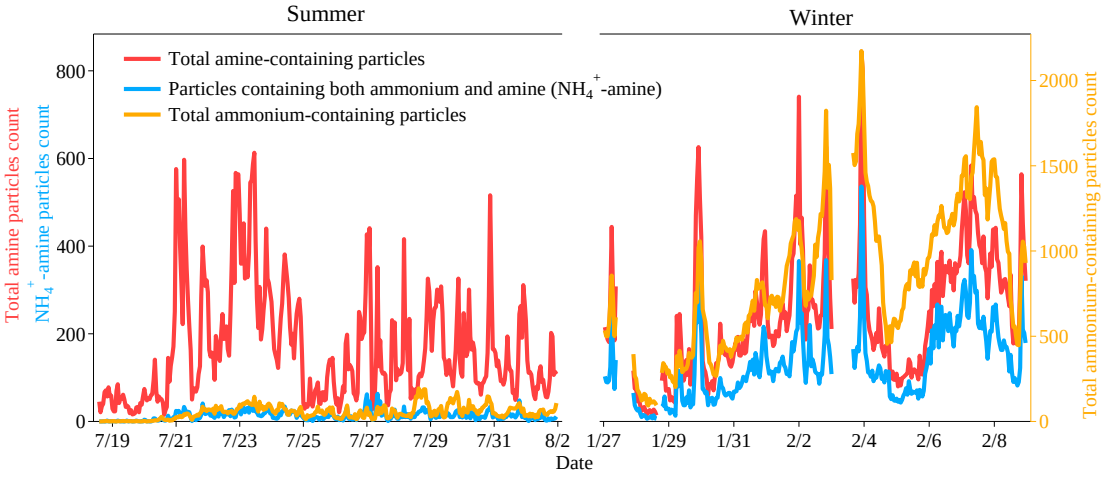


Figure 7. Temporal variations of total amine-containing particles, total ammonium-containing particles and particles containing both ammonium and amine ($NH_4^+$-amine) during sampling period in Heshan.

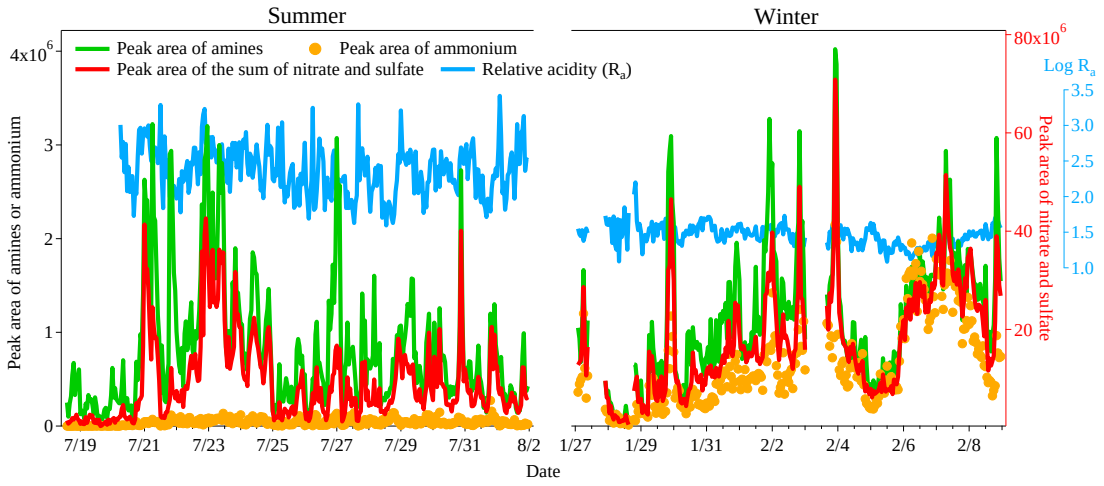


Figure 8. Temporal variations in the peak areas of amines, ammonium, and the sum of sulfate and nitrate in amine-containing particles during summer and winter. The relative acidity ratio ($R_a$), which was calculated as the ratio of the total sulfate and nitrate peak areas to the ammonium peak area, is plotted as log($R_a$).